Edinburgh Research Explorer

Myelin repair in vivo is increased by targeting oligodendrocyte precursor cells with nanoparticles encapsulating leukaemia inhibitory factor (LIF)

OPEN ACCESS

CrossMark

Myelin repair *in vivo* is increased by targeting oligodendrocyte precursor cells with nanoparticles encapsulating leukaemia inhibitory factor (LIF)

Sonja Rittchen [a], Amanda Boyd [a], Alasdair Burns [a], Jason Park [b], Tarek M. Fahmy [b], Su Metcalfe [c, **], Anna Williams [a, *]

[a] *Centre for Regenerative Medicine, University of Edinburgh, 5, Little France Drive, Edinburgh, EH16 4UU, UK*
[b] *Department of Biomedical Engineering, Department of Immunobiology, Yale School of Engineering and Applied Science and Yale School of Medicine, 55 Prospect Street, New Haven, CT, 06511, USA*
[c] *John van Geest Centre for Brain Repair, University of Cambridge, Addenbrooke's Hospital, Forvie Site, Robinson Way, Cambridge, CB2 0PY, UK*

ARTICLE INFO

ABSTRACT

Multiple sclerosis (MS) is a progressive demyelinating disease of the central nervous system (CNS). Many nerve axons are insulated by a myelin sheath and their demyelination not only prevents saltatory electrical signal conduction along the axons but also removes their metabolic support leading to irreversible neurodegeneration, which currently is untreatable. There is much interest in potential therapeutics that promote remyelination and here we explore use of leukaemia inhibitory factor (LIF), a cytokine known to play a key regulatory role in self-tolerant immunity and recently identified as a pro-myelination factor. In this study, we tested a nanoparticle-based strategy for targeted delivery of LIF to oligodendrocyte precursor cells (OPC) to promote their differentiation into mature oligodendrocytes able to repair myelin. Poly(lactic-co-glycolic acid)-based nanoparticles of ~120 nm diameter were constructed with LIF as cargo (LIF-NP) with surface antibodies against NG-2 chondroitin sulfate proteoglycan, expressed on OPC. *In vitro*, NG2-targeted LIF-NP bound to OPCs, activated pSTAT-3 signalling and induced OPC differentiation into mature oligodendrocytes. *In vivo*, using a model of focal CNS demyelination, we show that NG2-targeted LIF-NP increased myelin repair, both at the level of increased number of myelinated axons, and increased thickness of myelin per axon. Potency was high: a single NP dose delivering picomolar quantities of LIF is sufficient to increase remyelination.

Impact statement

Nanotherapy-based delivery of leukaemia inhibitory factor (LIF) directly to OPCs proved to be highly potent in promoting myelin repair *in vivo*: this delivery strategy introduces a novel approach to delivering drugs or biologics targeted to myelin repair in diseases such as MS.

© 2015 Published by Elsevier Ltd.

1. Introduction

There are no effective treatments of central nervous system (CNS) neurodegenerative diseases, and one block to progress in this field is effective systemic delivery of a therapeutic that crosses the blood–brain barrier (BBB) and targets specific CNS cells without off-target effects. One such disease is multiple sclerosis (MS), which affects 2.3 million people worldwide, often starts in young adulthood and is disabling, thus costing the economy an estimated 3 billion US dollars each year [1]. MS pathology consists of inflammatory demyelination of CNS axons causing neurological symptoms initially, when saltatory conduction for efficient nerve impulse conductance becomes compromised, and later compounded by the loss of metabolic support from myelinating oligodendrocytes leading to irreversible neurodegeneration. Although there are now effective immunomodulatory treatments that reduce

probability of new relapses [2], there are no treatments that reduce, slow or stop neurodegeneration and associated progressive disability.

One potential neuroprotective therapeutic strategy is to enhance repair of demyelination (remyelination), carried out by endogenous oligodendrocyte precursor cells (OPCs) recruited to the area of damage, and which differentiate into mature oligo-dendrocytes (OD) able to remyelinate axons (reviewed in Ref. [3]). However, in many MS lesions there appears to be a critical block in the maturation of OPCs to myelinating OD [4,5] and factors that improve OPC maturation improve remyelination in animal models of demyelination. Several such pro-maturation and pro-remyelination factors have been identified, but there are difficulties in translating these potential drug targets into practical therapies for patients, as these must cross the BBB to reach OPCs in the CNS, and ideally should be delivered directly to OPCs, to avoid off-target effects. Nanotechnology may solve these problems, by use of nanoparticles (NPs) that can cross the BBB, loaded with therapeutic cargo (drugs or biologics) and designed with surface-bound ligands that can be employed to target NPs to specific cells, providing local high concentrations of the cargo.

In this study, we test this potential solution of delivery of pro-remyelinating factors to the CNS using the known pro-remyelination factor leukaemia inhibitory factor (LIF) as cargo in poly(lactide-co-glycolide) (PLGA) nanoparticles, targeted using NG2 chondroitin sulphate proteoglycan antibodies to OPCs.

We chose to use LIF as a robust and accepted pro-remyelination factor as a proof of principle to test this novel delivery strategy. In rodents, LIF is well known to promote developmental myelination [6] and remyelination after demyelinating injury [7–10], by the mechanism of promoting OD maturation [11,12]. LIF is also known to play a key regulatory role in self-tolerant immunity, directly opposing IL-17 production [13], and IL-17 has been shown to inhibit OPC maturation in rodents [14]. In humans, LIF is detectable in the CSF of MS patients [15], in T cells and some macrophage/microglia found in MS lesions [16]. Therefore, overall, LIF is espe-cially attractive as a therapeutic candidate for the treatment of MS. Since LIF is rapidly degraded in vivo, and high doses may have unwanted off-target effects, we sought a method for its targeted delivery to OPCs using anti-NG2 chondroitin sulphate proteoglycan antibodies on the surface of modified biodegradable NP loaded with LIF.

We chose PLGA nanoparticles to provide a biocompatible and biodegradable material able to maintain both cargo stability and sustained, controlled release of cargo for a prolonged therapeutic effect [17]. In vivo, PLGA slowly degrades by hydrolysis to lactic acid and glycolic acid, monomeric derivatives that feed into metabolic pathways for eventual release as carbon dioxide and water. The degradation rate of these polymers, and often the corresponding cargo release rate, can vary from days (PGA) to months (PLA) and is easily manipulated by varying the ratio of PLA to PGA. For therapy, the physiologic compatibility of PLGA, PGA and PLA have been established as safe in humans; these materials have a history of over 30 years in various human clinical applications including drug delivery systems.

In our study, we then asked whether LIF formulated in PLGA NP targeted to OPC (i) attach to and induce OPC maturation into mature OD in vitro and (ii) improve reparative remyelination in vivo.

2. Materials and methods

Animal work was carried out in accordance with the University of Edinburgh regulations under Home Office rules, with local ethics committee consent. Animals/cells were randomly allocated a treatment group and data was analysed blinded to treatment group.

2.1. Nanoparticle production

Mouse LIF was encapsulated in avidin-coated PLGA nanoparticles (50:50 PLA:PGA) using a modified version of a previously described water/oil/water double emulsion technique [18]. Briefly, 50 μg LIF was dissolved in 200 μL PBS and added dropwise with vortexing to 100 mg PGLA in 2 ml dichloromethane. The resulting emulsion was added to 4 ml of aqueous surfactant solution containing 2.5 mg/ml PVA and 2.5 mg/ml avidin-palmitate bioconjugate (previously described [18]), and sonicated to create an emulsion containing nano-sized droplets of polymer/solvent, LIF and surfactant. Solvent was removed by magnetic stirring at room temperature; hardened NPs were then washed 3x in DI water and lyophilized for long-term storage. NP size and morphology were analysed via scanning electron microscopy (Philips XL30 system at 10 kV), and a Nanosight imaging/sizing system. Release of LIF was measured by incubating particles in PBS at 37°C and measuring LIF concen-trations in supernatant fractions by ELISA. To make targeted NP, they were resus-pended in 100 μl of biotinylated anti-NG2 antibody (1/2, rabbit, Millipore AB5320B) in phosphate buffered saline (PBS) and incubated at room temperature for 30 min to allow conjugation of anti-NG2 antibody to the avidin-coated NP. Antibody-coated NP were pelleted by centrifugation at 700 rpm for 2 min and excess antibody-containing supernatant collected and stored at 4°C for reuse up to 3 times. NP pellets were resuspended in 20 μl PBS to get a stock solution of 15 mg NP/ml. Serial dilutions in PBS were performed resulting in final concentrations in OPC culture of 300, 30 and 3 μg NP/ml.)

2.2. OPC culture and assays

OPC cultures were prepared from neonatal Sprague–Dawley rats as described [19]. In brief, mixed glial cultures were made from postnatal day1–2 rat pups and after 10 days isolated by shaking the cultures, relying on differential adhesion of OPCs compared to macrophages and astrocytes and resulting in cultures of 80–90% purity. OPCs were seeded on Poly-D-Lysine-coated chamber slides, and maintained in SATO medium at 37 °C in 7.5% CO₂. OPCs were then cultured in the presence of NPs – either targeted or non-targeted and containing LIF or empty, compared to negative control (medium only) or positive control (recombinant LIF at 100 U/ml obtained from in-house Hybridoma) and binding, activation, and their effect on proliferation, apoptosis and differentiation assessed.

To detect whether targeted NP bind to OPCs, we used either anti-rabbit fluo-rescent-tagged secondary antibody (1/1000, AlexaFluor®, Invitrogen) to bind to the anti-NG2 antibody attached to the NP surface, or streptavidin conjugated to a fluorescent tag (which binds to the avidin on the surface) (1/1000, AlexaFluor®, Invitrogen).

To determine whether LIF was being released and having an effect on signalling within the OPCs, we made use of its downstream signalling molecule STAT3, which is phosphorylated and moves to the nucleus when the LIF receptor is activated and is detectable using antibodies specific for phosphorylated STAT3 at the TYR705 residue (species: mouse, 1/100, Cell Signalling Technology 9131).

Survival was assessed by culturing OPCs in basic media lacking both serum and growth factors (DMEM (Gibco 41966-029)) for 24 h in the presence of each of the four types of NP by TUNEL assay (Invitrogen Click-iT TUNEL Alexa Fluor Imaging Assay).

Proliferation was assessed by culturing OPCs in basic media (DMEM, as above) containing 0.5% fetal calf serum but no growth factors in the presence of each of the four types of NP for 24 h, in the presence of EdU (Invitrogen Click-iT EdU imaging kit), which incorporates into the DNA of dividing cells.

Differentiation of OPCs was assessed by incubation with NP for 24 h and then the media refreshed and differentiation assessed after 4 days in culture, by assessment of myelin basic protein expression (MBP) (species: rat, 1/300 Serotec MCA409S) by immunofluorescence staining as MBP is a main protein component of the myelin sheath and a marker of mature oligodendrocytes, and staining immature OPC with anti-NG2 antibody (species: mouse, 1/100, Millipore MAB5384).

All cultures were fixed with 4% PFA for immunofluorescence analysis. Confocal z-stacks were acquired using Leica SPE confocal microscope with a x40 lens, using Leica acquisition software, and analysed using Image J software. For all experiments we carried out 3 experiments (from 3 separate rat litters) with duplicates for each treatment in each. We quantified a minimum of 250 OPCs per condition, from 4 to 8 non-overlapping images. For statistical significance, we used a two-way ANOVA with Bonferroni multi comparison post-test, with p < 0.05 considered significant.

2.3. Method for stereotactic surgery and tissue processing

We made focal demyelinating lesions in mouse corpus callosum by stereotactic injection of the myelin toxin lysophosphatidylcholine(LPC) and then injected either LIF-containing NG2 targeted NPs, LIF-containing non-targeted NPs or empty NG2-targeted NPs into the lesion at day 8, aiming to accelerate the maturation of OPCs which have already migrated into the lesion into myelinating oligodendrocytes. Using anaesthetized 12-week-old C57Bl/6 male mice, 2 μl of 1% w/v LPC was injected through a hole drilled in the skull at stereotactic coordinates 1.2 mm posterior, 0.5 mm lateral, 1.4 mm deep to the bregma over 4 min using a 30 gauge needle attached to a Hamilton syringe, driven by a KD Scientific Nano pump, which was left in situ for 4 min to reduce backflow. On Day 8, we injected 2 μl of the lowest

concentration of NP that had an effect on OPC differentiation *in vitro* (3 μg/ml) in a similar manner, using the same coordinates. Mice were perfused with 2% glutaraldehyde/4% Paraformaldehyde (PFA) at day 18 or day 25 after initial lesion. Fixed brains were cut into 1-mm thick coronal section samples, post-fixed in 4% PFA containing 0.5% glutaraldehyde for 1 h, then 2% PFA/2% glutaraldehyde at 4 °C overnight and processed into resin blocks using standard protocols. Sagittal 1 μm semi-thin sections were cut on a Reichert OMU4 ultramicrotome were stained with toluidine blue to select suitable areas for investigation. Ultra-thin sections, 90 nm thick, were stained in uranyl acetate and lead citrate and visualised using a Philips CM120 Transmission electron microscope. Images were taken with a Gatan Orius CCD camera.

2.4. Measurements and statistics

We used the gold standard method of detection and measurement of remyelination − measurement of both the percentage of myelinated fibres within a lesion and the thickness of the myelin sheaths by electron microscopy. To count the percentage of myelinated fibres in the lesion, we took ten photographs from random, non-overlapping fields within each lesion, accounting for at least 1000 axons per

mouse, with 5 mice per group (n = 5), and analysed blinded to the treatment group. To measure g-ratios, we traced the axonal circumference and the whole fibre circumference (using a graphics pad and pen) of all myelinated axons in 5 non-overlapping random fields within the lesion (at least 100 axons per mouse), and divided the two values. Again we used 5 mice per group (n = 5), and analysed the data blinded to the treatment group. We analysed the data using two-way ANOVA with Bonferroni multi comparison post-test with p < 0.05 considered significant.

3. Results

3.1. LIF-NP promote differentiation of oligodendrocytes

LIF-NPs were prepared as detailed in Methods. These NPs have typical spherical morphology (Fig. 1a) and a tight size distribution with a mean diameter of 126 nm ± 50 s. d. (Fig. 1b). LIF molecules are embedded within the PLGA matrix and thus protected from
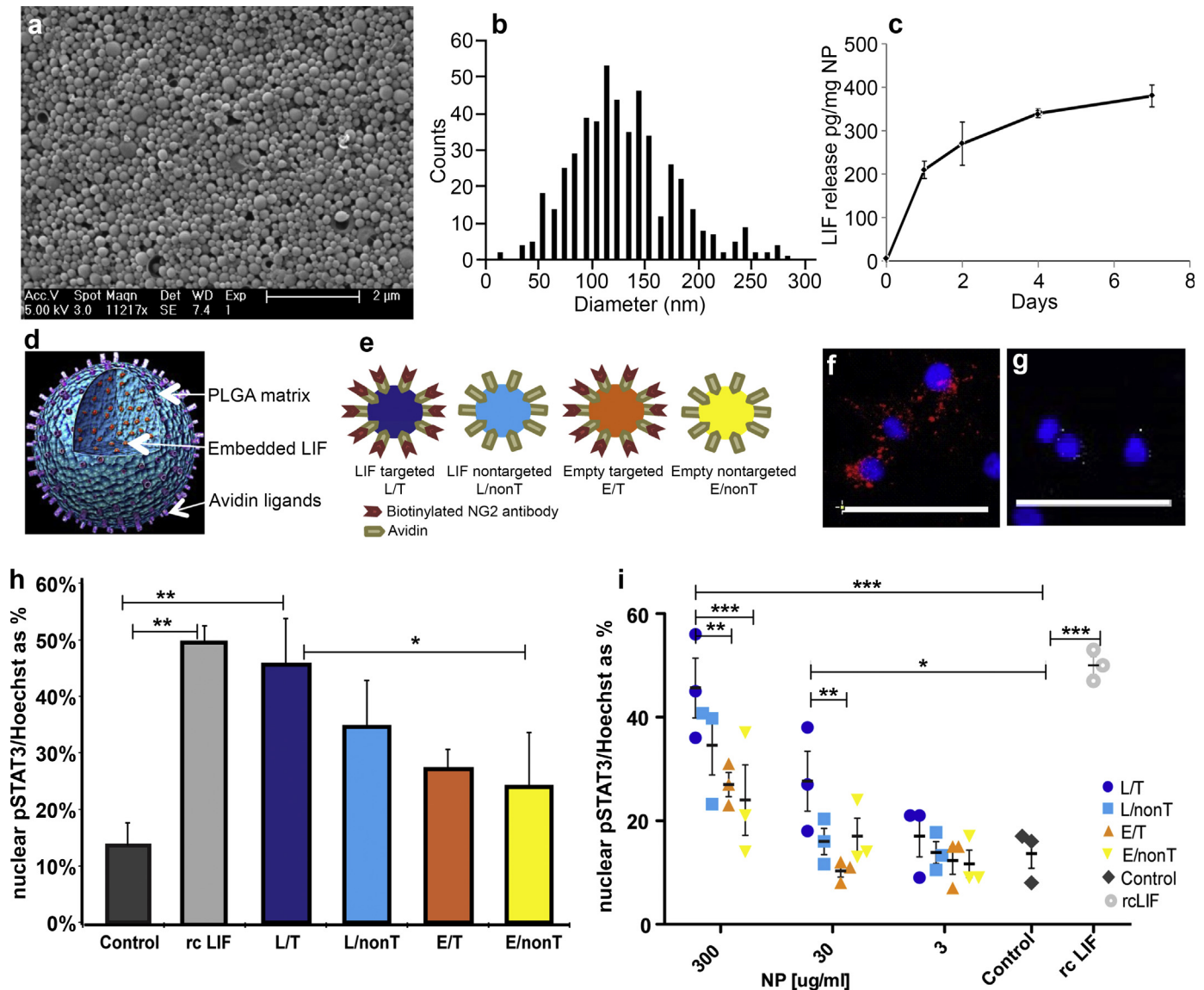

Fig. 1. STAT-3 signalling in OPC is activated by LIF-NP. Physical properties of LIF-NP according to morphology (a), size (b) and release rate of LIF(c). (d) Cartoon of composition of PLGA-based NP with embedded LIF and surface avidin for attachment of biotinylated targeting antibody. (e) Four types of NP used. (f) NP with attached biotinylated anti-NG2 antibody bind to purified OPC, as shown using anti-rabbit secondary antibodies (red) but non-targeted NPs (without this surface antibody), do not bind OPC (g) (as shown by sparse staining by anti-streptavidin antibodies against surface avidin (white)). Blue = Hoechst staining of nuclei. Scale bar: 50 μm (h) Histogram showing significant increases in nuclear phospho-STAT-3 at 24 h incubation with targeted LIF-NP (at 300 μg/ml). (i) Dose response curves at 24 h show that targeted LIF-NP has greatest potency for STAT-3 activation. (For h and i, Two-way ANOVA with Bonferroni multi comparison post-test; *p < 0.05, **p < 0.01, ***p < 0.001; mean ± SEM, n = 3 experiments in duplicate). (For interpretation of the references to colour in this figure legend, the reader is referred to the web version of this article.)

degradation that normally limits LIF's plasma half-life *in vivo* to a few minutes. LIF cargo release during PLGA matrix degradation showed an initial burst, then prolonged kinetics over several days (Fig. 1c) [20,21]. The surface avidin molecules allow attachment of biotinylated anti-NG2 antibodies, to target OPCs (as illustrated in Fig. 1d). This allows multiple targeting ligands per NP ensuring high valency and avidity of contact together with delivery of multiple LIF molecules per biorecognition event to ensure relatively high concentration of cytokine within the microenvironment of the targeted cell while avoiding systemic exposure to the therapeutic cytokine. Accordingly, our nanoparticulate approach to target LIF met our need for controlled, sustained release of bioactive LIF in low, physiological doses within the OPC microenvironment.

Next we determined the effect of these LIF-NP when targeted to NG2+ OPCs by preparing purified primary rat OPCs and assigning these to six treatment groups: *Group 1*: untreated controls; *Group 2*: recombinant LIF (positive control) (100 U/ml); *Group 3*: NG2-targeted LIF-NP (300 μg/ml); *Group 4*: non-targeted LIF-NP (300 μg/ml); *Group 5*: NG2-targeted empty-NP (300 μg/ml); and *Group 6*: non-targeted empty-NP (300 μg/ml) (illustrated in Fig. 1e). After confirming NG2-specific attachment of the NG2-targeted NP to isolated rat OPC (Fig. 1f and g), the different therapeutic groups were cultured for 24 h then stained for nuclear phospho-STAT-3 as a surrogate marker of LIF-induced signal transduction [22].

Compared to untreated controls, both recombinant LIF and NG2-targeted LIF-NP induced over fourfold increase in nuclear phospho-STAT-3 staining, significantly greater than in NP groups 4, 5, and 6 (Fig. 1h). Significant dose-dependent effects were seen, confirming the greatest potency of the NG2-targeted LIF-NP (Fig. 1i). This positive effect of NG2-targeted LIF-NP on nuclear localisation of pSTAT3 was maintained over 4 days in culture (after treatment with NPs for the first 24 h) where OPCs were allowed to mature into oligodendrocytes (suppl. Fig. 1).

We concluded that LIF-NP released bioactive LIF and that targeting to OPC increased LIF-mediated activation of intracellular signal transduction to the nucleus for activation of LIF response genes. This bioactivity is in accordance with previous studies where LIF-NP targeted to CD4+ T lymphocytes induced the transcription factor Foxp3 required for immune self-tolerance [21].

We next asked if signalling induced by LIF-NP treatment resulted in improved OPC biological function. *In vivo*, for remyelination to occur, an OPC must survive, proliferate, and differentiate: accordingly each aspect was assessed in isolated rat OPCs in response to NP treatment. Supplementary Fig. 2 shows that both survival and proliferation measured after 24 h of NP treatment were equivalent across all NP groups. However, differentiation (as assessed by myelin basic protein (MBP)-positive cells) was increased by treatment with NG2-targeted LIF-NP (Fig. 2a and
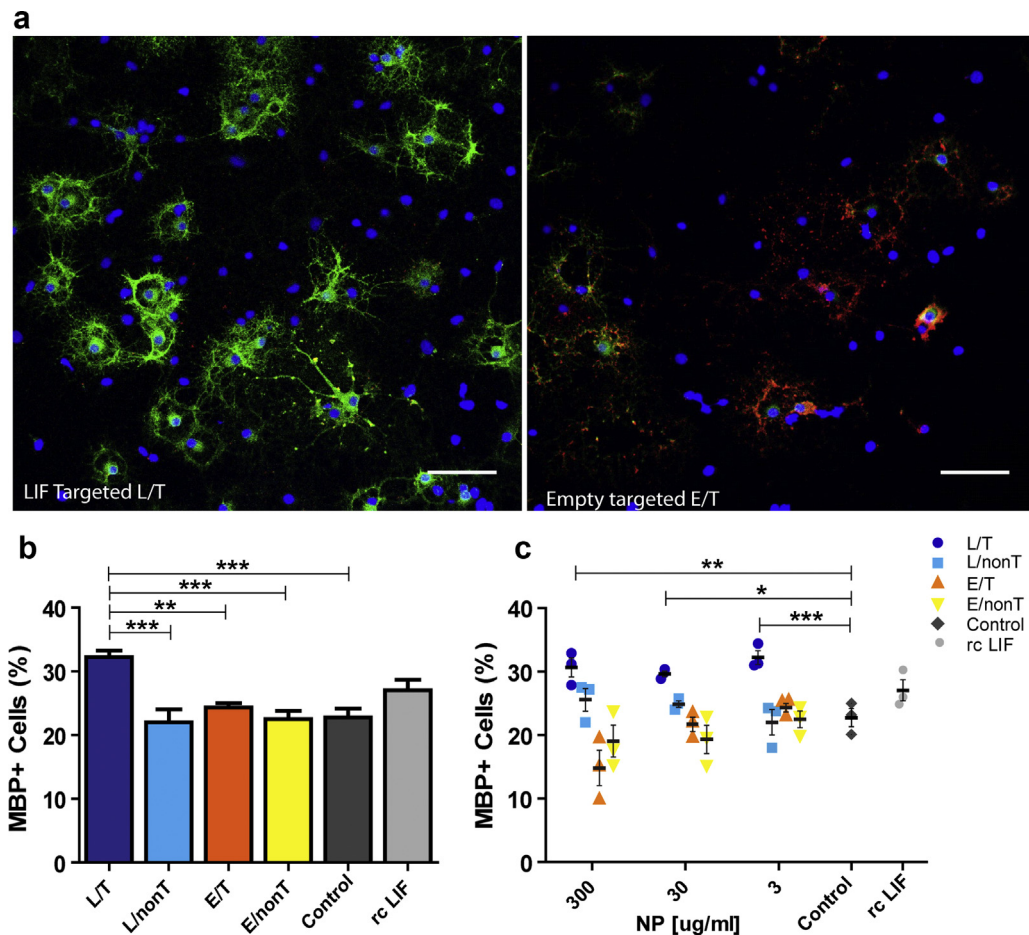

Fig. 2. OPC mature into OD in response to NG2-targeted LIF-NP. (a) The number of MBP + mature OD in 4d cultures of OPC following initial treatment with targeted LIF-NP for 24 h increases after treatment with NG2-targeted LIF-NP compared to empty targeted NP. (OPC − labelled with NG2 (red), OD labelled with MBP (green), blue (Hoechst) = nuclei. Scale bars:50 μm (b) The percentage of MBP + OD at 4d after treatment with 3 μg/ml NP during the first 24 h, compared to no treatment (negative control), or recombinant LIF (positive control). (c) Dose response curves of 300, 30, and 3 μg/ml NP, compared to controls as above. (b and c: Two-way ANOVA with Bonferroni multicomparison post-test; *p < 0.05, **p < 0.01, ***p < 0.001; mean ± SEM, n = 3 experiments in duplicate). (For interpretation of the references to colour in this figure legend, the reader is referred to the web version of this article.)

Supplementary Fig. 3). In these experiments, OPC were treated with NPs for 24 h, then cultured for 72 h in fresh growth medium. Targeted LIF-NP treatment significantly increased the number of MBP + ODs, in contrast to non-targeted LIF-NP, targeted empty-NP and untreated controls (Fig. 2b). This confirms requirement for both (i) LIF cargo and (ii) targeting to NG2+ cells to achieve enhanced OPC maturation. The NP dose–response experiments (Fig. 2c) revealed high potency of the NG2-targeted LIF-NP where, even at the lowest dose tested − 3 μg LIF-NP/ml, ~33% of the cells differentiated into MBP + OD.

Calculation of LIF-NP potency was based on the release data by 2 days of 300 pg LIF from 1 mg of NP (Fig. 1c) i.e. 3 μg LIF-NP/ml equates to ~0.9 pg LIF/ml. The potency for inducing differentiation measured at 4 days was higher than for nuclear pSTAT-3 localisation at 24 h where 3 μg/ml targeted LIF-NP lacked significant effect, possibly due to delivery of physiologically relevant doses of LIF over the longer 72 h sustaining signalling cues to OPC for their functional differentiation to OD. Evidence to support this is shown in Supplementary Fig. 1, where 3 μg/ml targeted LIF-NP treatment also showed increased pSTAT3 nuclear localisation in oligodendroglial cells cultured for 4 days.

3.2. LIF-NP enhance reparative remyelination in vivo

Next we examined if LIF-NP, as well as promoting OPC differentiation in vitro, can also promote remyelination in vivo within the CNS. The simplest model of demyelination in the mouse brain is stereotactic injection of the myelin toxin lysophosphatidylcholine (LPC) into the corpus callosum. This model has advantage over more complex models of CNS demyelination such as experimental autoimmune encephalomyelitis (EAE), where inflammation, demyelination and remyelination occur simultaneously. LPC produces a focal area of demyelination and remyelination with a defined timeline: demyelination by 3 days, migration of OPCs into the lesion starts at day 6 and differentiation of OPCs into ODs starts at day 10 with complete spontaneous remyelination by 4 weeks. Thus, to look for any reparative potential of LIF-NP, we introduced the NP directly into established lesions at 8d post LPC treatment − i.e. after OPC ingression but prior to their differentiation.

After lesioning, three treatment groups of mice were established, one receiving NG2-targeted LIF-NP, the second receiving non-targeted LIF-NP and the third containing NG2-targeted empty-NP: for each, 2 μl of 3 μg/ml NP suspension were infused into the lesion at identical stereotactic coordinates. This low NP dose was selected as a stringent test based on the high and specific potency of targeted LIF-NP for inducing OPC differentiation in vitro. Five mice of each group were culled at 18d and 25d post lesion (10d, or 17d post therapy) as outlined in Fig. 3 where representative states of myelination/demyelination/remyelination are also illustrated. To quantify remyelination, we used the gold standard method of measurement of both the percentage of myelinated axons within the lesioned area and the myelin thickness relative to axon diameter (g-ratio) by electron microscopy. The g-ratio of a normal mature myelinated axon is constant at ~0.7 since myelin thickness is tightly regulated according to axon size. In the context of remyelination, g-ratios approaching 1.0 reflect thinner and less mature myelin. The experimental data in Fig. 4 shows representative electron micrographs taken 18d and 25d post lesion for the
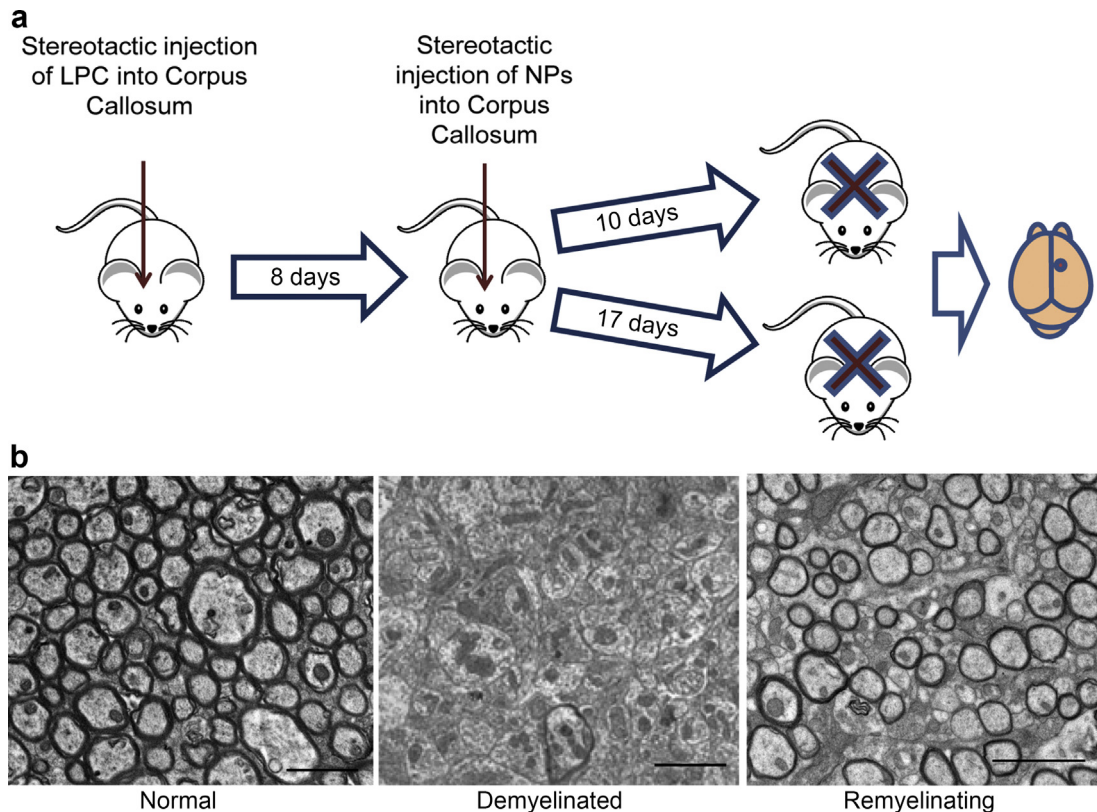

Fig. 3. Experimental design measuring effect of LIF-NP on *in vivo* remyelination. (a) Schematic showing the experimental timeline: LPC lesion (day 0) followed by treatment with either targeted LIF-NP or targeted empty-NP (day 8) (2 μl of a 3 μg/ml solution). Mice were culled at either day 18 or 25 and the lesioned site processed for electron microscopy. (b) Representative cross-sectional electron microscopy images of normal myelinated, demyelinated, and remyelinating corpus callosum. (The remyelinating image is a low power view of Fig. 4a E/T 18dpl).
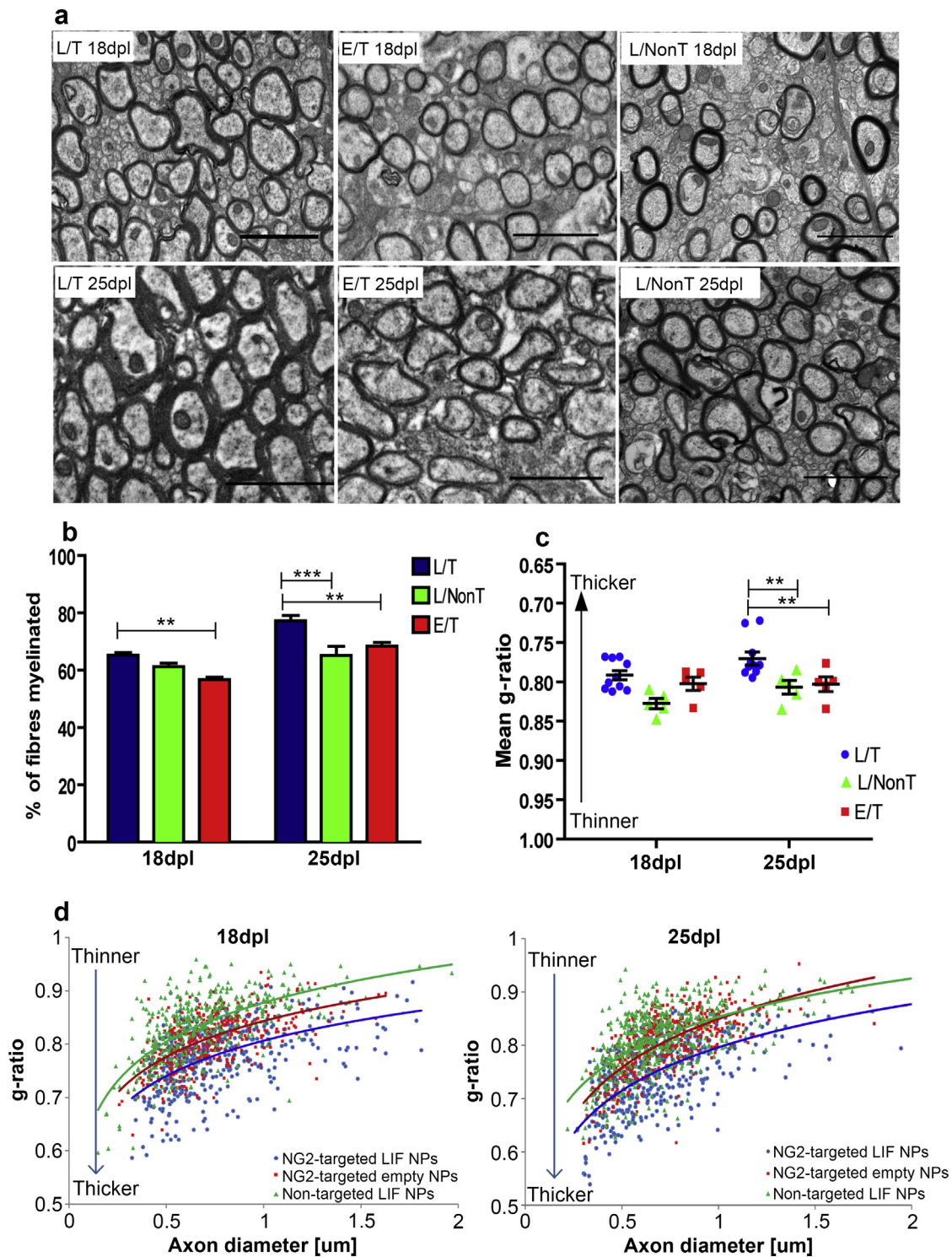
Fig. 4. NG2-targeted LIF-NP promote thicker myelin and increased numbers of myelinated axons during myelin repair. (a) Electron micrographs show increased remyelination in lesions treated with targeted LIF-NP compared to non-targeted LIF-NP or targeted empty-NP. Scale bars:2 μm (b) The percentage of myelinated fibres within the lesion area is significantly higher in targeted LIF-NP treated animals (L/T), at 25 dpl, compared to non-targeted LIF-NP (L/NonT) or targeted empty-NP treated animals (E/T). (mean ± SEM, n = 5 mice per group, number of axons counted/mouse >1000. Two-way ANOVA with Bonferroni multicomparison post-test **p > 0.01, ***p > 0.001). (c) The mean g-ratio (axon perimeter/myelinated fibre perimeter) is significantly lower (thicker myelin) in targeted LIF-NP (L/T) treated mice compared to non-targeted LIF-NP (L/NonT) or targeted empty-NP (E/T) treated mice at 25dpl (mean ± SEM, n = 5 mice per group, number of myelinated axons measured/mouse > 100. Two-way ANOVA with Bonferroni multicomparison post-test **p < 0.01). (d) Scatter plots showing the correlation of g-ratio and axon diameter for each axon measured at 18 and 25 d, with superimposed logarithmic trendline. (blue = NG2-targeted LIF-NP therapy, green = non-targeted LIF-NP therapy, red = NG2-targeted empty-NP therapy;. Note y-axis reversed compared to (c). (For interpretation of the references to colour in this figure legend, the reader is referred to the web version of this article.)

three experimental groups (Fig. 4a). The percentage of myelinated fibres per lesion was significantly higher in the NG2-targeted LIF-NP group (L/T) compared to either the empty-NP (E/T) group or the non-targeted LIF-NP (L/NonT) group at 25 days post lesion (Fig. 4b). Furthermore, myelin was significantly thicker in those animals receiving LIF-NP compared to empty-NP or non-targeted LIF-NP at 25 days post lesion, both seen as an average g-ratio (Fig. 4c) and with the scatter plot where each axon g-ratio is plotted against its axon diameter (Fig. 4d). No adverse effects were seen in any of the treated mice, and those treated with NG2-targeted empty-NP or non-targeted LIF-NP showed a normal trajectory for remyelination as seen in untreated controls of this model's historical controls. Thus, NG2-targeted and non-targeted LIF-NP were well tolerated whilst the enhanced trajectory of remyelination using NG2-targeted LIF-NP required both NG2-targeting and LIF cargo.

CNS remyelination in rodents is significantly more efficient than in humans, in that the percentage of fibres remyelinated after demyelinating injury returns to normal (~80% in the mouse corpus callosum) although the thickness of the myelin sheath remains thinner. Thus, we believe that acceleration of remyelination to this extent with significantly faster normalization of the percentage of myelinated fibres in the lesion and significantly thicker, more mature myelin is also biologically significant.

4. Discussion

We have shown that, in vitro, NG2-targeted LIF-NP bind to OPCs and the bioactivity of encapsulated LIF was retained, shown by activation of STAT-3 signalling pathways downstream of the LIF receptor, together with promotion of OPC maturation into mature oligodendrocytes. In vivo, we have shown that NG2-targeted LIF-NP improve CNS remyelination both in terms of the percentage of fibres remyelinated and their thickness (maturity of sheath): proof of principle that this novel delivery strategy is efficacious for myelin repair and as such holds promise for treatment of diseases such as MS. Notably the concentration of NP with therapeutic efficacy in vivo occurred using 2 μl of 3 μg/ml NP which equates to around 1.8 fg of LIF, and taking a molecular weight of LIF as 20kD, this equates to therapeutic efficacy at 9×10^{-20} mol. This high potency was unexpected. However, there is precedent for a potent effect of cytokines when delivered from biodegradable particles or cells interacting in close proximity. Indeed, a recent mathematical model estimated that potency of a drug or cytokine can be increased by several orders of magnitude when the cytokine is delivered via a biodegradable particle targeted to T cells [23,24]. We cannot be sure that all of our effect is a result of LIF acting directly on OPCs, as these cells in lesions are closely surrounded by astrocytes and macrophages, which although do not express NG2, express LIF receptors [25,26] and the action of astrocytes and macrophages can also influence remyelination [27,28]. However, the lack of effect shown by using non-targeted LIF-NP (of the same concentration) suggests that this effect is dependent on targeted delivery of LIF to cells using NG2 antibodies. We added NP intralesionally, as proof of concept confirming the powerful potential of this delivery system as a targeted approach to deliver bioactive molecules for in situ myelin repair. For translation into clinical use it is notable that NP delivered intravenously can cross the BBB [29,30], at least in rodents, or can be delivered intranasally directly to the CNS [31,32] bypassing the BBB, supporting the concept that intravenous or intranasal delivery of LIF-NP targeted to NG2 may promote remyelination of demyelinated lesions. Moreover, the nanoparticle platform used here is already in clinical trials (e.g. Clinicaltrials.gov NCT01812746, NCT01792479).

5. Conclusion

Our experimental approach confirms potent efficacy of LIF-NP for myelin repair in mice in vivo. This paves the way for a new era in therapeutic delivery of drugs or biologics (including LIF) targeted to potently improve the function of OPCs and enhance CNS remyelination in MS patients. Furthermore, combinations of drugs and biologics may even be co-encapsulated within the same delivery NP, ensuring either simultaneous or even sequential delivery of pertinent factors controlling OPC behaviour in myelin repair.

Appendix A. Supplementary data

Supplementary data related to this article can be found at http://dx.doi.org/10.1016/j.biomaterials.2015.03.044.

References

[1] Ma VY, Chan L, Carruthers KJ. Incidence, prevalence, costs, and impact on disability of common conditions requiring rehabilitation in the United States: stroke, spinal cord injury, traumatic brain injury, multiple sclerosis, osteoarthritis, rheumatoid arthritis, limb loss, and back pain. Archives Phys Med Rehabilitation 2014;95(5):986–95. e1.

[2] Broadley SA, Barnett MH, Boggild M, Brew BJ, Butzkueven H, Heard R, et al. Therapeutic approaches to disease modifying therapy for multiple sclerosis in adults: an Australian and New Zealand perspective part 2 new and emerging therapies and their efficacy. J Clin Neurosci 2014. http://dx.doi.org/10.1016/j.jocn.2014.01.018. pii: S0967–5868(14)00184-2.

[3] Münzel EJ, Williams A. Promoting remyelination in multiple sclerosis-recent advances. Drugs 2013;73(18):2017–29.

[4] Lucchinetti C, Bruck W, Parisi J, Scheithauer B, Rodriguez M, Lassmann H. A quantitative analysis of oligodendrocytes in multiple sclerosis lesions. A study of 113 cases. Brain 1999;122(Pt 12):2279–95.

[5] Chang A, Tourtellotte WW, Rudick R, Trapp BD. Premyelinating oligodendrocytes in chronic lesions of multiple sclerosis. N Engl J Med 2002;346(3):165–73.

[6] Ishibashi T, Lee PR, Baba H, Fields RD. Leukemia inhibitory factor regulates the timing of oligodendrocyte development and myelination in the postnatal optic nerve. J Neurosci Res 2009;87(15):3343–55.

[7] Deverman BE, Patterson PH. Exogenous leukemia inhibitory factor stimulates oligodendrocyte progenitor cell proliferation and enhances hippocampal remyelination. J Neurosci 2012;32(6):2100–9.

[8] Butzkueven H, Zhang JG, Soilu-Hanninen M, Hochrein H, Chionh F, Shipham KA, et al. LIF receptor signaling limits immune-mediated demyelination by enhancing oligodendrocyte survival. Nat Med 2002;8(6):613–9.

[9] Slaets H, Hendriks JJ, Van den Haute C, Coun F, Baekelandt V, Stinissen P, et al. CNS-targeted LIF expression improves therapeutic efficacy and limits autoimmune-mediated demyelination in a model of multiple sclerosis. Mol Ther 2010;18(4):684–91.

[10] Laterza C, Merlini A, De Feo D, Ruffini F, Menon R, Onorati M, et al. iPSC-derived neural precursors exert a neuroprotective role in immune-mediated demyelination via the secretion of LIF. Nat Commun 2013;4:2597.

[11] Mayer M, Bhakoo K, Noble M. Ciliary neurotrophic factor and leukemia inhibitory factor promote the generation, maturation and survival of oligodendrocytes in vitro. Development 1994;120(1):143–53.

[12] Fischer R, Wajant H, Kontermann R, Pfizenmaier K, Maier O. Astrocyte-specific activation of TNFR2 promotes oligodendrocyte maturation by secretion of leukemia inhibitory factor. Glia 2014;62(2):272–83.

[13] Gao W, Thompson L, Zhou Q, Putheti P, Fahmy TM, Strom TB, et al. Treg versus Th17 lymphocyte lineages are cross-regulated by LIF versus IL-6. Cell Cycle 2009;8(9):1444–50.

[14] Kang Z, Wang C, Zepp J, Wu L, Sun K, Zhao J, et al. Act1 mediates IL-17-induced EAE pathogenesis selectively in NG2+ glial cells. Nat Neurosci 2013;16(10):1401–8.

[15] Mashayekhi F, Salehi Z. Expression of leukemia inhibitory factor in the cere-brospinal fluid of patients with multiple sclerosis. J Clin Neurosci 2011;18(7): 951–4.

[16] Vanderlocht J, Hellings N, Hendriks JJ, Vandenabeele F, Moreels M, Buntinx M, et al. Leukemia inhibitory factor is produced by myelin-reactive T cells from multiple sclerosis patients and protects against tumor necrosis factor-alpha-induced oligodendrocyte apoptosis. J Neurosci Res 2006;83(5):763–74.

[17] Metcalfe SM, Fahmy TM. Targeted nanotherapy for induction of therapeutic immune responses. Trends Mol Med 2012;18(2):72–80.

[18] Park J, Mattessich T, Jay SM, Agawu A, Saltzman WM, Fahmy TM. Enhance-ment of surface ligand display on PLGA nanoparticles with amphiphilic ligand conjugates. J Control Release 2011;156(1):109–15. official journal of the Controlled Release Society.

[19] McCarthy KD, de Vellis J. Preparation of separate astroglial and oligoden-droglial cell cultures from rat cerebral tissue. J Cell Biol 1980;85(3):890–902.

[20] Zhao JW, Dyson SC, Kriegel C, Tyers P, He X, Fahmy TM, et al. Modelling of a targeted nanotherapeutic 'stroma' to deliver the cytokine LIF, or XAV939, a potent inhibitor of Wnt-beta-catenin signalling, for use in human fetal dopaminergic grafts in Parkinson's disease. Dis Model Mech 2014;7:1–11.

[21] Park J, Gao W, Whiston R, Strom TB, Metcalfe S, Fahmy TM. Modulation of CD4+ T lymphocyte lineage outcomes with targeted, nanoparticle-mediated cytokine delivery. Mol Pharm 2011;8(1):143–52.

[22] Azari MF, Profyris C, Karnezis T, Bernard CC, Small DH, Cheema SS, et al. Leukemia inhibitory factor arrests oligodendrocyte death and demyelination in spinal cord injury. J Neuropathol Exp Neurol 2006;65(9):914–29.

[23] Steenblock ER, Fadel T, Labowsky M, Pober JS, Fahmy TM. An artificial antigen-presenting cell with paracrine delivery of IL-2 impacts the magnitude and direction of the T cell response. J Biol Chem 2011;286(40):34883–92.

[24] Labowsky M, Fahmy TM. Diffusive transfer between two intensely interacting cells with limited surface kinetics. Chem Eng Sci 2012;74:114–23.

[25] Getchell TV, Shah DS, Partin JV, Subhedar NK, Getchell ML. Leukemia inhibi-tory factor mRNA expression is upregulated in macrophages and olfactory receptor neurons after target ablation. J Neurosci Res 2002;67(2):246–54.

[26] Fan YY, Zhang JM, Wang H, Liu XY, Yang FH. Leukemia inhibitory factor in-hibits the proliferation of primary rat astrocytes induced by oxygen-glucose deprivation. Acta Neurobiol Exp 2013;73(4):485–94.

[27] Miron VE, Boyd A, Zhao JW, Yuen TJ, Ruckh JM, Shadrach JL, et al. M2 microglia and macrophages drive oligodendrocyte differentiation during CNS remyeli-nation. Nat Neurosci 2013;16(9):1211–8.

[28] Williams A, Piaton G, Lubetzki C. Astrocytes–friends or foes in multiple sclerosis? Glia 2007;55(13):1300–12.

[29] Tosi G, Fano RA, Bondioli L, Badiali L, Benassi R, Rivasi F, et al. Investigation on mechanisms of glycopeptide nanoparticles for drug delivery across the blood-brain barrier. Nanomedicine (Lond) 2011;6(3):423–36.

[30] Tosi G, Bondioli L, Ruozi B, Badiali L, Severini GM, Biffi S, et al. NIR-labeled nanoparticles engineered for brain targeting: in vivo optical imaging appli-cation and fluorescent microscopy evidences. J Neural Transm 2011;118(1): 145–53.

[31] Gambaryan PY, Kondrasheva IG, Severin ES, Guseva AA, Kamensky AA. Increasing the efficiency of parkinson's disease treatment using a poly(lactic-co-glycolic acid) (PLGA) based L-DOPA delivery system. Exp Neurobiol 2014;23(3):246–52.

[32] Seju U, Kumar A, Sawant KK. Development and evaluation of olanzapine-loaded PLGA nanoparticles for nose-to-brain delivery: in vitro and in vivo studies. Acta Biomater 2011;7(12):4169–76.